PROCEEDINGS OF SCIENCE

PoS(LATTICE2024)433

# 2024 Update on $\varepsilon_K$ with lattice QCD inputs

**Seungyeob Jwa,**[a,*] **Jeehun Kim,**[a] **Sunghee Kim,**[a] **Sunkyu Lee,**[b] **Weonjong Lee,**[a,1] **Jaehoon Leem**[c] **and Sungwoo Park**[d]

[a] *Lattice Gauge Theory Research Center, CTP, and FPRD, Department of Physics and Astronomy, Seoul National University, Seoul 08826, South Korea*

[b] *Center for Precision Neutrino Research (CPNR), Department of Physics, Chonnam National University, Yongbong-ro 77, Puk-gu, Gwangju 61186, Korea*

[c] *Computational Science and Engineering Team, Innovation Center, Samsung Electronics, Hwaseong, Gyeonggi-do 18448, South Korea.*

[d] *Lawrence Livermore National Lab, 7000 East Ave, Livermore, CA 94550, USA*

*E-mail:* `wlee@snu.ac.kr`

We report recent progress on $\varepsilon_K$ evaluated directly from the standard model (SM) with lattice QCD inputs such as $\hat{B}_K$, exclusive $|V_{cb}|$, $|V_{us}|$, $|V_{ud}|$, $\xi_0$, $\xi_2$, $\xi_{\text{LD}}$, $f_K$, and $m_c$. We find that the standard model with exclusive $|V_{cb}|$ and lattice QCD inputs describes only $2/3 \cong 65\%$ of the experimental value of $|\varepsilon_K|$ and does not explain its remaining 35%, which represents a strong tension in $|\varepsilon_K|$ at the $5.1\sigma \sim 4.1\sigma$ level between the SM theory and experiment. We also find that this tension disappears when we use the inclusive value of $|V_{cb}|$ obtained using the heavy quark expansion based on the QCD sum rule approach. We also report results for $|\varepsilon_K|$ obtained using the Brod-Gorbahn-Stamou (BGS) method for $\eta_i$ of $u - t$ unitarity, which leads to even a stronger tension of $5.7\sigma \sim 4.2\sigma$ with lattice QCD inputs.

*The 41st International Symposium on Lattice Field Theory (LATTICE2024)*
*28 July - 3 August 2024*
*Liverpool, UK*

---

[1] For the SWME collaboration

[*] Speaker

https://pos.sissa.it/

PoS(LATTICE2024)433

## 1. Introduction

This paper is an update of our previous reports [1–9]. We report recent progress in the determination of $|\varepsilon_K|$ with updated inputs from lattice QCD. Updated input parameters include $\lambda$, $\bar{\rho}$, $\bar{\eta}$, exclusive $|V_{cb}|$, $|V_{us}|$, $|V_{ud}|$, $|V_{us}|/|V_{ud}|$, $M_W$, $m_c(m_c)$, and $M_t$ (the pole mass of top quarks).

Here we adopt the same color convention as that in our previous papers [1–9] in Tables 1–6. We use `red` for new input data used to evaluate $\varepsilon_K$. We use `blue` for new input data which is not used.

## 2. Input parameters: Wolfenstein parameters

We summarize results for $|V_{ud}|$, $|V_{us}|$, and $\dfrac{|V_{us}|}{|V_{ud}|}$ from lattice QCD in table 1.

| type | $\lvert V_{us}\rvert$ | $\lvert V_{ud}\rvert$ | Ref. |
|---|---|---|---|
| $N_f = 2+1+1$ | 0.22483(61) | 0.97439(14) | FLAG-24 [10]p79t20 |
| $N_f = 2+1$ | 0.22481(58) | 0.97440(13) | FLAG-24 [10]p79t20 |

**(a)** $|V_{us}|$ and $|V_{ud}|$ from lattice QCD

| type | $\lvert V_{us}\rvert/\lvert V_{ud}\rvert$ | Ref. |
|---|---|---|
| $f_{K^\pm}/f_{\pi^\pm}$ | 0.23126(50) | FLAG-24 [10]p75 |
| $f_K/f_\pi$ | 0.23131(45) | FLAG-24 [10]p76 |

**(b)** $|V_{us}|/|V_{ud}|$ from lattice QCD

**Table 1:** (a) $|V_{us}|$ and $|V_{ud}|$ (b) $|V_{us}|/|V_{ud}|$.

$$\lambda = \frac{|V_{us}|}{\sqrt{|V_{ud}|^2 + |V_{us}|^2}} = \frac{r}{\sqrt{1+r^2}}\,, \qquad r = \frac{|V_{us}|}{|V_{ud}|} \tag{1}$$

Using Eq. (1), we determine $\lambda$ from the ratio $r = |V_{us}|/|V_{ud}|$, since it has less error than that obtained directly from $|V_{us}|$ and $|V_{ud}|$. We present results for $\lambda$ in Table 2. We also summarize recent update on $\bar{\rho}$ and $\bar{\eta}$ of Wolfenstein parameters (WP) in Table 2. When we evaluate $|\varepsilon_K|$, we use the angle-only-fit (AOF) results in Table 2 to avoid the unwanted correlations between $(\varepsilon_K, |V_{cb}|)$, and $(\bar{\rho}, \bar{\eta})$, as explained in Ref. [5, 9]. We determine the parameter $A$ directly from $|V_{cb}|$. We also present results of the CKM-fitter [11] (2021) and the UTfit [12, 13](2022-2023) in Table 2 for comparison.

| WP | CKMfitter | | UTfit | | AOF | |
|---|---|---|---|---|---|---|
| $\lambda$ | $0.22498^{+0.00023}_{-0.00021}$ | [11] | 0.22519(83) | [12, 13] | 0.22536(42) | [10] |
| $\bar{\rho}$ | $0.1562^{+0.0112}_{-0.0040}$ | [11] | 0.160(9) | [13, 14] | 0.159(16) | [14] |
| $\bar{\eta}$ | $0.3551^{+0.0051}_{-0.0057}$ | [11] | 0.346(9) | [13, 14] | 0.339(10) | [14] |

**Table 2:** Wolfenstein parameters

## 3. Input parameters: $|V_{cb}|$

We present recent results for exclusive $|V_{cb}|$ and inclusive $|V_{cb}|$ in Table 3. In Table 3 (a), the results for exclusive $|V_{cb}|$ obtained by various groups of lattice QCD are summarized: FNAL/MILC, FLAG, HFLAV, and HPQCD. Here `BGL` denotes a kind of the parametrization methods for data

| channel | value | method | ref | source |
|---|---|---|---|---|
| $B \to D^* \ell \bar{\nu}$ | 38.40(78) | BGL | [18] p27e76 | FNAL/MILC-22 |
| ex-comb | 39.46(53) | comb | [10]p181e282 | FLAG-24 |
| ex-comb | 39.10(50) | comb | [19] p120e221 | HFLAV-23 |
| ex-comb | 39.03(56)(67) | comb | [20] p24e50 | HPQCD-23 |

**(a)** Exclusive $|V_{cb}|$ in units of $1.0 \times 10^{-3}$.

| scheme | value | ref | source |
|---|---|---|---|
| kinetic scheme | 42.16(51) | [21] p1 | Gambino-21 |
| 1S scheme | 41.98(45) | [19] p108e200 | 1S-23 |

**(b)** Inclusive $|V_{cb}|$ in units of $1.0 \times 10^{-3}$.

**Table 3:** Results for (a) exclusive $|V_{cb}|$ and (b) inclusive $|V_{cb}|$. The abbreviation p27e76 means Eq. (76) on page 27.

analysis [5, 15], and `comb` represents combined results from various groups for multiple decay channels. They are consistent with one another within $1.0\sigma$ uncertainty. We also present recent results for inclusive $|V_{cb}|$ in Table 3 (b). There are a number of attempts to determine inclusive $|V_{cb}|$ from lattice QCD, but all of them at present belong to the category of exploratory study rather than that of precision calculation [16, 17].

## 4. Input parameter $\xi_0$

The absorptive part of long distance effects on $\varepsilon_K$ is parametrized by $\xi_0$.

$$\xi_0 = \frac{\text{Im}\, A_0}{\text{Re}\, A_0}, \qquad \xi_2 = \frac{\text{Im}\, A_2}{\text{Re}\, A_2}, \qquad \text{Re}\left(\frac{\varepsilon'}{\varepsilon}\right) = \frac{\omega}{\sqrt{2}|\varepsilon_K|}(\xi_2 - \xi_0)\,. \tag{2}$$

In lattice QCD, we can determine $\xi_0$ by two independent methods: the direct and indirect methods. In the direct method, one determines $\xi_0$ by combining the lattice QCD results for $\text{Im}\, A_0$ with experimental results for $\text{Re}\, A_0$. In the indirect method, one determines $\xi_0$ using Eq. (2) with lattice QCD results for $\xi_2$ combined with experimental results for $\varepsilon'/\varepsilon$, $\varepsilon_K$, and $\omega$.

We summarize experimental results for $\text{Re}\, A_0$ and $\text{Re}\, A_2$, lattice results for $\text{Im}\, A_0$ and $\text{Im}\, A_2$ calculated by RBC-UKQCD in Table 4. We also present results for $\xi_0$ in Table 4. Here we use the results of the indirect method for $\xi_0$ to evaluate $\varepsilon_K$, since the total errors are much smaller than those of the direct method.

## 5. Input parameters: $\hat{B}_K$, $\xi_{\text{LD}}$, and others

The FLAG 2024 [10] reports results for $\hat{B}_K$ in lattice QCD for $N_f = 2$, $N_f = 2+1$, and $N_f = 2+1+1$. Here we use the results for $\hat{B}_K$ with $N_f = 2+1$, which is obtained by taking an average over the five data points from BMW 11, Laiho 11, RBC-UKQCD 14, SWME 14, and RBC-UKQCD 24 presented in Table 5 (a).

| parameter | method | value | Ref. | source |
|---|---|---|---|---|
| Re $A_0$ | exp | $3.3201(18) \times 10^{-7}$ GeV | [22**?** , 23] | NA |
| Re $A_2$ | exp | $1.4787(31) \times 10^{-8}$ GeV | [22] | NA |
| $\omega$ | exp | $0.04454(12)$ | [22] | NA |
| $\lvert\varepsilon_K\rvert$ | exp | $2.228(11) \times 10^{-3}$ | [24] p285e13.46a | PDG-2024 |
| Re $(\varepsilon'/\varepsilon)$ | exp | $1.66(23) \times 10^{-3}$ | [24] p285e13.46b | PDG-2024 |
| parameter | method | value ( GeV) | Ref. | source |
| Im $A_0$ | lattice/G-parity BC | $-6.98(62)(144) \times 10^{-11}$ | [25] p4t1 | RBC-UK-2020 |
| Im $A_0$ | lattice/periodic BC | $-8.7(12)(26) \times 10^{-11}$ | [26] p30e70 | RBC-UK-2023 |
| Im $A_2$ | lattice/G-parity BC | $-8.34(103) \times 10^{-13}$ | [25] p31e90 | RBC-UK-2020 |
| Im $A_2$ | lattice/periodic BC | $-5.91(13)(175) \times 10^{-13}$ | [26] p30e68 | RBC-UK-2023 |
| parameter | method | value | Ref | source |
| $\xi_0$ | indirect | $-1.738(177) \times 10^{-4}$ | [25] | SWME |
| $\xi_0$ | direct | $-2.102(472) \times 10^{-4}$ | [25] | SWME |

**(a)** Results for $\xi_0$ obtained using the direct and indirect methods in lattice QCD.

**Table 4:** Results for $\xi_0$. Here, we use the same notation as in Table 3. The abbreviation p4t1 means Table 1 on page 4.

The dispersive long distance (LD) effect $\xi_{\rm LD}$ is

$$\xi_{\rm LD} = \frac{m'_{\rm LD}}{\sqrt{2}\Delta M_K}\,, \qquad m'_{\rm LD} = -\mathrm{Im}\left[\mathcal{P}\sum_{C}\frac{\langle\overline{K}^0|H_{\rm w}|C\rangle\langle C|H_{\rm w}|K^0\rangle}{m_{K^0}-E_C}\right] \tag{3}$$

There are two independent methods to estimate $\xi_{\rm LD}$: one is the BGI estimate [32], and the other is the RBC-UKQCD estimate [33, 34], which ex explained in Ref. [5]. In the BGI method, one estimates $\xi_{\rm LD}$ using chiral perturbation theory, using Eq. (4).

$$\xi_{\rm LD} = -0.4(3) \times \frac{\xi_0}{\sqrt{2}} \tag{4}$$

In the RBC-UKQCD method, one estimates $\xi_{\rm LD}$ using Eq. (5).

$$\xi_{\rm LD} = (0 \pm 1.6)\% \quad \text{of} \quad |\varepsilon_K|^{\rm SM}. \tag{5}$$

Here we use both methods to estimate the sie of $\xi_{\rm LD}$.

| Collaboration | Ref. | $\hat{B}_K$ |
|---|---|---|
| RBC/UKQCD 24 | [27] | 0.7436(25)(78) |
| SWME 15 | [28] | 0.735(5)(36) |
| RBC/UKQCD 14 | [29] | 0.7499(24)(150) |
| Laiho 11 | [30] | 0.7628(38)(205) |
| BMW 11 | [31] | 0.7727(81)(84) |
| FLAG-24 | [10] p96e111 | 0.7533(91) |

**(a)** $\hat{B}_K$

| Input | Value | Ref. |
|---|---|---|
| $G_F$ | $1.1663788(6) \times 10^{-5}$ GeV$^{-2}$ | PDG-24 [24] p137t1.1 |
| $\theta$ | $43.52(5)°$ | PDG-24 [24] p284e13.42 |
| $m_{K^0}$ | 497.611(13) MeV | PDG-24 [24] p40 |
| $\Delta M_K$ | $3.484(6) \times 10^{-12}$ MeV | PDG-24 [24] p41 |
| $F_K$ | 155.7(3) MeV | FLAG-24 [10] p80e80 |
| $m_c(m_c)$ | 1.278(6) GeV | FLAG-24 [10] p56e53 |
| $m_t(m_t)$ | 162.77(27)(17) GeV | PDG-24 [24] p1379 |
| $M_W$ | 80.353(6) GeV | SM-2024 [24] p815,s54p3 |

**(b)** Other parameters

**Table 5:** (a) Results for $\hat{B}_K$ and (b) other input parameters.

In Table 5 (b), we present other input parameters needed to evaluate $\varepsilon_K$. We present the charm quark mass $m_c(m_c)$ and the top quark mass $m_t(m_t)$ in Table 5 (b). Since the lattice results of various groups with $N_f = 2+1+1$ shows some inconsistency among them, we take the results for $m_c(m_c)$ with $N_f = 2+1$ from FLAG 2024 [10]. To obtain $m_t(m_t)$, we take results for the pole mass $M_t$ from PDG 2024 [24]. Here we use the standard model predition (SM-2024) result for $M_W$ [24] to evaluate $\varepsilon_K$.

## 6. Input parameters: Higher order QCD corrections

We summarize higher order QCD corrections $\eta_i$ in Table 6. There are two sets of $\eta_i$: one is $\eta_i$ of $c-t$ unitarity (the traditional method [5, 6], Table 6 (a)), and the other is $\eta_i$ of $u-t$ unitarity (the BGS method [35], Table 6 (b)). The BGS method ($\eta_{ut}^{\text{BGS}}$) are supposed to have better convergence with respect to the charm quark mass contribution [35].

| Input | Value | Ref. |
|---|---|---|
| $\eta_{cc}$ | 1.72(27) | [6] |
| $\eta_{tt}$ | 0.5765(65) | [36] |
| $\eta_{ct}$ | 0.496(47) | [37] |

**(a)** $\eta_i$ of $c-t$ unitarity

| Input | Value | Ref. |
|---|---|---|
| $\eta_{tt}^{\text{BGS}}$ | $0.55(1 \pm 4.2\% \pm 0.1\%)$ | [35] |
| $\eta_{ut}^{\text{BGS}}$ | $0.402(1 \pm 1.3\% \pm 0.2\% \pm 0.2\%)$ | [35] |

**(b)** $\eta_i^{\text{BGS}}$ of $u-t$ unitarity

**Table 6:** QCD corrections: (a) the traditional method ($\eta_i$ of $c-t$ unitarity), and (b) the BGS method ($\eta_i$ of $u-t$ unitarity).

## 7. Results for $|\varepsilon_K|^{\text{SM}}$

Here we presents results for $|\varepsilon_K|^{\text{SM}}$ evaluated using various combinations of input parameters. We report results for $|\varepsilon_K|^{\text{SM}}_{c-t}$ calculated using the traditional method with $\eta_i$ of $c-t$ unitarity in Subsection 7.1, and $|\varepsilon_K|^{\text{SM}}_{u-t}$ calculated using the BGS method with $\eta_i$ of $u-t$ unitarity in Subsection 7.2. Here the superscript $^{\text{SM}}$ represents the theoretical expectation value of $|\varepsilon_K|$ obtained directly from the SM, and the subscript $_{c-t}$ ($_{u-t}$) represents that obtained using the traditional method with $\eta_i$ of $c-t$ unitarity (the BGS method of $\eta_i$ of $u-t$ unitarity).

### 7.1 $\eta_i$ of $c-t$ unitarity (the traditional method)

In Fig. 1 (a), we present results of $|\varepsilon_K|^{\text{SM}}_{c-t}$ calculated directly from the standard model (SM) with the lattice QCD inputs using the traditional method for $\eta_i$ of $c-t$ unitarity. Here the blue curve represents the theoretical results for $|\varepsilon_K|^{\text{SM}}_{c-t}$ obtained using the FLAG-24 results for $\hat{B}_K$, the AOF results for Wolfenstein parameters, the FNAL/MILC-22 results for exclusive $|V_{cb}|$, results for $\xi_0$ with the indirect method, results for $\eta_i$ of $c-t$ unitarity (the traditional method), and the RBC-UKQCD estimate for $\xi_{\text{LD}}$. The red curve in Fig. 1 represents the experimental results for $|\varepsilon_K|^{\text{Exp}}$. Here the superscript $^{\text{Exp}}$ represents experimental results for $|\varepsilon_K|$.

In Table 7, we summarize our results for $|\varepsilon_K|^{\text{SM}}_{c-t}$ and $\Delta\varepsilon_K = |\varepsilon_K|^{\text{Exp}} - |\varepsilon_K|^{\text{SM}}$. We present results for $|\varepsilon_K|^{\text{SM}}_{c-t}$ obtained using the RBC-UKQCD estimate for $\xi_{\text{LD}}$ in Table 7 (a), and those

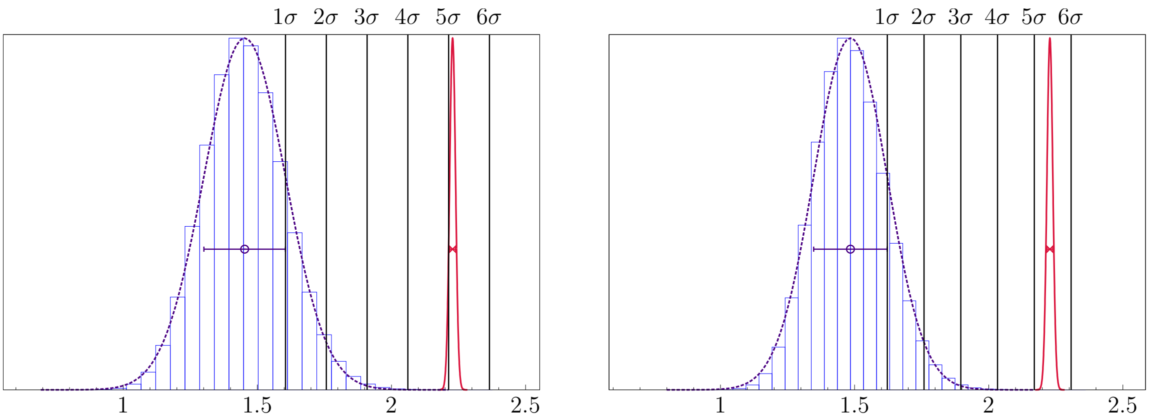

**(a)** $|\varepsilon_K|^{\text{SM}}_{c-t}$ **(b)** $|\varepsilon_K|^{\text{SM}}_{u-t}$

**Figure 1:** $|\varepsilon_K|^{\text{SM}}$ with exclusive $|V_{cb}|$ (FNAL/MILC-22) in units of $1.0 \times 10^{-3}$: (a) $|\varepsilon_K|^{\text{SM}}$ with $\eta_i$ of $c - t$ unitarity (the traditional method), and (b) $|\varepsilon_K|^{\text{SM}}$ with $\eta_i$ of $u - t$ unitarity (the BGS method).

obtained using the BGI estimate for $\xi_{\text{LD}}$ in Table 7 (b). In Table 7, we find that the theoretical expectation values of $|\varepsilon_K|^{\text{SM}}_{c-t}$ with lattice QCD inputs (including exclusive $|V_{cb}|$) have $5.1\sigma \sim 4.1\sigma$ tension with the experimental value of $|\varepsilon_K|^{\text{Exp}}$, while there is no tension with inclusive $|V_{cb}|$ obtained using the heavy quark expansion and QCD sum rules.

In Fig. 2 (a), we present the time evolution of $\Delta\varepsilon_K/\sigma$ during the period of 2012–2024. In 2012, $\Delta\varepsilon_K$ was $2.5\sigma$, but now it is $5.1\sigma$ with exclusive $|V_{cb}|$ (FNAL/MILC-22). We use the FNAL/MILC-22 results for exclusive $|V_{cb}|$ as a representative sample, since it contains the most comprehensive analysis of the $\bar{B} \to D^* \ell \bar{\nu}$ decays at both zero recoil and non-zero recoil, while it incorporates experimental results of both BELLE and BABAR, and independent of data merging with unwanted correlation. In Fig. 2 (b) we present the time evolution of the average $\Delta\varepsilon_K$ and the error $\sigma_{\Delta\varepsilon_K}$ during the same period.

In Table 8 (a), we present the error budget for $|\varepsilon_K|^{\text{SM}}_{c-t}$. Here we find that $|V_{cb}|$ gives the largest error ($\approx$ 52%), while $\eta_{ct}$, $\bar{\eta}$, and $\eta_{cc}$ are subdominant in the error budget. Hence, it is essential

| $\lvert V_{cb}\rvert$ | method | source | $\lvert\varepsilon_K\rvert^{\text{SM}}_{c-t}$ | $\Delta\varepsilon_K$ |
|---|---|---|---|---|
| exclusive | BGL | FNAL/MILC-22 | $1.453 \pm 0.152$ | $5.10\sigma$ |
| exclusive | comb | HFLAV-23 | $1.551 \pm 0.133$ | $5.10\sigma$ |
| exclusive | comb | FLAG-24 | $1.605 \pm 0.138$ | $4.50\sigma$ |
| exclusive | comb | HPQCD-23 | $1.544 \pm 0.169$ | $4.06\sigma$ |
| inclusive | 1S | 1S-23 | $2.017 \pm 0.155$ | $1.36\sigma$ |
| inclusive | kinetic | Gambino-21 | $2.050 \pm 0.162$ | $1.10\sigma$ |

**(a)** $|\varepsilon_K|^{\text{SM}}_{c-t}$ with RBC-UKQCD estimate for $\xi_{\text{LD}}$

| $\lvert V_{cb}\rvert$ | method | reference | $\lvert\varepsilon_K\rvert^{\text{SM}}_{c-t}$ | $\Delta\varepsilon_K$ |
|---|---|---|---|---|
| exclusive | BGL | FNAL/MILC-22 | $1.501 \pm 0.155$ | $4.70\sigma$ |
| exclusive | comb | HFLAV-23 | $1.599 \pm 0.135$ | $4.64\sigma$ |

**(b)** $|\varepsilon_K|^{\text{SM}}_{c-t}$ with BGI estimate for $\xi_{\text{LD}}$

**Table 7:** $|\varepsilon_K|$ in units of $1.0 \times 10^{-3}$, and $\Delta\varepsilon_K = |\varepsilon_K|^{\text{Exp}} - |\varepsilon_K|^{\text{SM}}_{c-t}$ in units of $\sigma$.

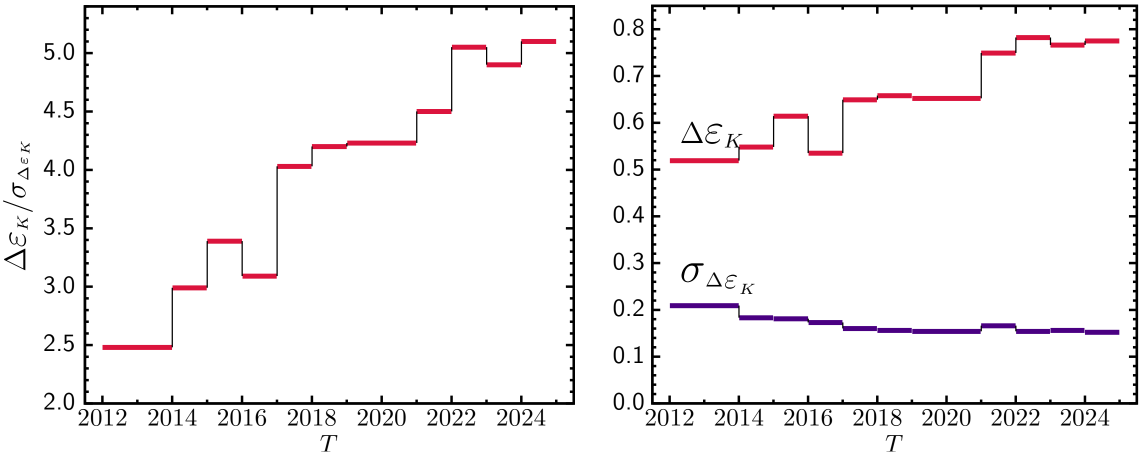

**(a)** Time evolution of $\Delta\varepsilon_K/\sigma_{\Delta\varepsilon_K}$

**(b)** Time evolution of the average and error of $\Delta\varepsilon_K$

**Figure 2:** Chronicle of (a) $\Delta\varepsilon_K/\sigma_{\Delta\varepsilon_K}$, and (b) $\Delta\varepsilon_K$ and $\sigma_{\Delta\varepsilon_K}$.

to reduce the errors in $|V_{cb}|$ as much as possible. Part of the errors in exclusive $|V_{cb}|$ come from experiments in BELLE, BELLE2, BABAR, and LHCb, which are beyond our control, but will decrease thanks to on-going accumulation of higher statistics in BELLE2 and LHCb. Part of the errors in exclusive $|V_{cb}|$ come from the theory used to evaluate the semi-leptonic form factors for $\bar{B} \to D^{(*)}\ell\bar{\nu}$ decays, using tools in lattice QCD.

### 7.2 $\eta_i$ of $u - t$ unitarity (the BGS method)

In Fig. 1 (b), we present results for $|\varepsilon_K|^{\rm SM}_{u-t}$ obtained directly from the SM using the BGS method for $\eta_i$ of $u - t$ unitarity, the FLAG-24 results for $\hat{B}_K$, the AOF results for Wolfenstein parameters, the FNAL/MILC-22 results for exclusive $|V_{cb}|$, results for $\xi_0$ with the indirect method, the RBC-UKQCD estimate for $\xi_{\rm LD}$, and so on. In Table 9, we present results for $|\varepsilon_K|^{\rm SM}_{u-t}$ and its $\Delta\varepsilon_K$ obtained using the BGS method. Here we find a mismatch $\delta\varepsilon_K^{\rm BGS}$ in the central values (CV) for $|\varepsilon_K|^{\rm SM}$ between the traditional method and the BGS method for $\eta_i$: $\delta\varepsilon_K^{\rm BGS} \equiv |\varepsilon_K|^{\rm SM}_{u-t} - |\varepsilon_K|^{\rm SM}_{c-t}$. This mismatch comes from a number of small and tiny approximations introduced in the BGS method [35]. Here we count this CV mismatch $\delta\varepsilon_K^{\rm BGS}$ as an additional error, and add it to the total error in quadrature. Hence, the total error is $\sigma_t^{\rm BGS} = \sqrt{[\sigma_1^{\rm BGS}]^2 + [\delta\varepsilon_K^{\rm BGS}]^2}$, where $\sigma_t^{\rm BGS}$ represents the total error, and $\sigma_1^{\rm BGS}$ represents the errors coming from the input parameters. In Table 9, we present $\sigma_1^{\rm BGS}$, $\delta\varepsilon_K^{\rm BGS}$, and $\sigma_t^{\rm BGS}$ to demonstrate some sense on numerical size of them.

| source | error (%) | memo |
|---|---|---|
| $\lvert V_{cb}\rvert$ | 51.9 | exclusive |
| $\eta_{ct}$ | 21.9 | $c-t$ Box |
| $\bar{\eta}$ | 9.4 | AOF |
| $\eta_{cc}$ | 9.3 | $c-c$ Box |
| $\xi_{\rm LD}$ | 2.2 | RBC/UKQCD |
| $\bar{\rho}$ | 2.0 | AOF |
| $\hat{B}_K$ | 1.6 | FLAG-24 |
| ⋮ | ⋮ | ⋮ |

**(a)** Error budget for $|\varepsilon_K|^{\rm SM}_{c-t}$

| source | error (%) | memo |
|---|---|---|
| $\lvert V_{cb}\rvert$ | 63.1 | exclusive |
| $\bar{\eta}$ | 12.0 | AOF |
| $\eta_{tt}^{\rm BGS}$ | 10.7 | BGS |
| $\delta\varepsilon_K^{\rm BGS}$ | 5.4 | CV mismatch |
| $\xi_{\rm LD}$ | 2.9 | RBC/UKQCD |
| $\bar{\rho}$ | 2.2 | AOF |
| $\hat{B}_K$ | 2.0 | FLAG-24 |
| ⋮ | ⋮ | ⋮ |

**(b)** Error budget for $|\varepsilon_K|^{\rm SM}_{u-t}$

**Table 8:** Error budget table for $|\varepsilon_K|^{\rm SM}$ with (a) the traditional method ($\eta_i$ of $c-t$ unitarity), and (b) the BGS method ($\eta_i$ of $u-t$ unitarity).

| $\lvert V_{cb}\rvert$ | method | source | $\lvert\varepsilon_K\rvert^{\text{SM}}_{u-t}$ | $\sigma_1^{\text{BGS}}$ | $\delta\varepsilon_K^{\text{BGS}}$ | $\sigma_t^{\text{BGS}}$ | $\Delta\varepsilon_K/\sigma$ |
|---|---|---|---|---|---|---|---|
| excl | BGL | FNAL-MILC-22 | 1.484 | 0.133 | 0.032 | 0.137 | 5.43 |
| excl | comb | HFLAV-23 | 1.582 | 0.110 | 0.031 | 0.114 | 5.65 |
| excl | comb | FLAG-24 | 1.635 | 0.116 | 0.030 | 0.120 | 4.93 |
| excl | comb | HPQCD-23 | 1.575 | 0.151 | 0.031 | 0.154 | 4.24 |
| incl | 1S | 1S-23 | 2.043 | 0.131 | 0.026 | 0.134 | 1.37 |
| incl | kinetic | Gambino-21 | 2.075 | 0.140 | 0.025 | 0.142 | 1.07 |
| $\lvert\varepsilon_K\rvert^{\text{Exp}}$ | exp | PDG-24 | 2.228 |  |  | 0.011 | 0.00 |

**Table 9:** $\lvert\varepsilon_K\rvert^{\text{SM}}_{u-t}$ in units of $1.0\times10^{-3}$ obtained using the FLAG-24 results for $\hat{B}_K$, AOF for the Wolfenstein parameters, the `indirect` method for $\xi_0$, the `RBC-UKQCD` estimate for $\xi_{\text{LD}}$, and the `BGS` method for $\eta_i$ ($=\eta_i^{\text{BGS}}$) of $u-t$ unitarity.

From Table 9, we find that the theoretical results for $\lvert\varepsilon_K\rvert^{\text{SM}}_{u-t}$ obtained using lattice QCD inputs including exclusive $\lvert V_{cb}\rvert$ have $5.7\sigma \sim 4.2\sigma$ tension with the experimental results for $\lvert\varepsilon_K\rvert^{\text{Exp}}$, while the tension disappears for those obtained using inclusive $\lvert V_{cb}\rvert$ from heavy quark expansion and QCD sum rules.

In Table 8 (b), we present the error budget for $\lvert\varepsilon_K\rvert^{\text{SM}}_{u-t}$. Here we find that the error from exclusive $\lvert V_{cb}\rvert$ is dominant ($\approx 63\%$), while those errors from $\bar{\eta}$, $\eta_{tt}^{\text{BGS}}$, and $\delta\varepsilon_K^{\text{BGS}}$ are subdominant in the error budget. Hence, it is essential to reduce the errors of exclusive $\lvert V_{cb}\rvert$ as much as possible.

Due to lack of space, a large portion of interesting results for $\lvert\varepsilon_K\rvert^{\text{SM}}$ and $\Delta\varepsilon_K$ could not be presented in Tables 7 and 9: for example, results for $\lvert\varepsilon_K\rvert^{\text{SM}}_{c-t}$ obtained using exclusive $\lvert V_{cb}\rvert$ (FLAG-24) with the BGI estimate for $\xi_{\text{LD}}$, results for $\lvert\varepsilon_K\rvert^{\text{SM}}_{c-t}$ obtained using $\xi_0$ determined by the direct method, and so on. We plan to report them collectively in Ref. [38].

In order to reduce the errors in exclusive $\lvert V_{cb}\rvert$ on the theoretical side, there is an on-going project to determine $\lvert V_{cb}\rvert$ using the Oktay-Kronfeld (OK) action for the heavy quarks to calculate the form factors for $\bar{B} \to D^{(*)}\ell\bar{\nu}$ decays [39–47].

## Acknowledgments

We thank J. Bailey, Y.C. Jang, S. Sharpe, and R. Gupta for helpful discussion. We thank G. Martinelli for providing us with the most updated results of the UTfit Collaboration in time. The research of W. Lee is supported by the Mid-Career Research Program (Grant No. NRF-2019R1A2C2085685) of the NRF grant funded by the Korean government (MSIT). W. Lee would like to acknowledge the support from the KISTI supercomputing center through the strategic support program for the supercomputing application research (No. KSC-2018-CHA-0043, KSC-2020-CHA-0001, KSC-2023-CHA-0010, KSC-2024-CHA-0002). Computations were carried out in part on the DAVID cluster at Seoul National University.

## References

[1] S. Jwa, J. Kim, S. Kim, S. Lee, W. Lee, J. Leem et al., *2023 update of $\varepsilon_K$ with lattice QCD inputs*, *PoS* **LATTICE2023** (2024) 160 [`2312.02986`].

[2] SWME collaboration, *2022 update on $\varepsilon_K$ with lattice QCD inputs*, *PoS* **LATTICE2022** (2023) 297 [2301.12375].

[3] SWME collaboration, *2021 update on $\varepsilon_K$ with lattice QCD inputs*, *PoS* **LATTICE2021** (2021) 078 [2202.11473].

[4] LANL-SWME collaboration, *2019 update of $\varepsilon_K$ with lattice QCD inputs*, *PoS* **LATTICE2019** (2019) 029 [1912.03024].

[5] J.A. Bailey, S. Lee, W. Lee, J. Leem and S. Park, *Updated evaluation of $\epsilon_K$ in the standard model with lattice QCD inputs*, *Phys. Rev. D* **98** (2018) 094505 [1808.09657].

[6] SWME collaboration, *Standard Model evaluation of $\varepsilon_K$ using lattice QCD inputs for $\hat{B}_K$ and $V_{cb}$*, *Phys. Rev. D* **92** (2015) 034510 [1503.05388].

[7] J.A. Bailey, S. Lee, W. Lee, Y.-C. Jang, J. Leem and S. Park, *2018 Update on $\varepsilon_K$ with lattice QCD inputs*, *PoS* **LATTICE2018** (2018) 284 [1810.09761].

[8] SWME collaboration, *Update on $\varepsilon_K$ with lattice QCD inputs*, *EPJ Web Conf.* **175** (2018) 14015 [1710.06614].

[9] J.A. Bailey, Y.-C. Jang, W. Lee and S. Park, *Determination of $\varepsilon_K$ using lattice QCD inputs*, *PoS* **LATTICE2015** (2015) 348 [1511.00969].

[10] Flavour Lattice Averaging Group (FLAG) collaboration, *FLAG Review 2024*, 2411.04268.

[11] L. Vale Silva, *2023 update of the extraction of the CKM matrix elements*, in *12th International Workshop on the CKM Unitarity Triangle* [2405.08046].

[12] UTfit collaboration, *New UTfit Analysis of the Unitarity Triangle in the Cabibbo-Kobayashi-Maskawa scheme*, *Rend. Lincei Sci. Fis. Nat.* **34** (2023) 37 [2212.03894].

[13] UTfit collaboration, *The Unitarity Triangle Fit in the Standard Model and Hadronic Parameters from Lattice QCD: A Reappraisal after the Measurements of $\Delta m_s$ and $BR(B \to \tau\nu_\tau)$*, *JHEP* **10** (2006) 081 [hep-ph/0606167].

[14] M. Bona et al., *Overview and theoretical prospects for CKM matrix and CP violation from the UTfit Collaboration*, *PoS* **WIFAI2023** (2024) 007.

[15] C.G. Boyd, B. Grinstein and R.F. Lebed, *Precision corrections to dispersive bounds on form-factors*, *Phys. Rev. D* **56** (1997) 6895 [hep-ph/9705252].

[16] A. Barone, A. Jüttner, S. Hashimoto, T. Kaneko and R. Kellermann, *Inclusive semi-leptonic $B_{(s)}$ mesons decay at the physical b quark mass*, *PoS* **LATTICE2022** (2023) 403 [2211.15623].

[17] A. Barone, S. Hashimoto, A. Jüttner, T. Kaneko and R. Kellermann, *Approaches to inclusive semileptonic* $B_{(s)}$*-meson decays from Lattice QCD*, *JHEP* **07** (2023) 145 [`2305.14092`].

[18] Fermilab Lattice, MILC collaboration, *Semileptonic form factors for* $B \to D^* \ell \nu$ *at nonzero recoil from* $2+1$*-flavor lattice QCD: Fermilab Lattice and MILC Collaborations*, *Eur. Phys. J. C* **82** (2022) 1141 [`2105.14019`].

[19] Heavy Flavor Averaging Group, HFLAV collaboration, *Averages of b-hadron, c-hadron, and* $\tau$*-lepton properties as of 2021*, *Phys. Rev. D* **107** (2023) 052008 [`2206.07501`].

[20] HPQCD, (HPQCD Collaboration)‡ collaboration, $B \to D^*$ *and* $B_s \to D_s^*$ *vector, axial-vector and tensor form factors for the full* $q^2$ *range from lattice QCD*, *Phys. Rev. D* **109** (2024) 094515 [`2304.03137`].

[21] M. Bordone, B. Capdevila and P. Gambino, *Three loop calculations and inclusive Vcb*, *Phys. Lett. B* **822** (2021) 136679 [`2107.00604`].

[22] T. Blum et al., $K \to \pi\pi$ $\Delta I = 3/2$ *decay amplitude in the continuum limit*, *Phys. Rev. D* **91** (2015) 074502 [`1502.00263`].

[23] RBC, UKQCD collaboration, *Standard Model Prediction for Direct CP Violation in* $K{\to}\pi\pi$ *Decay*, *Phys. Rev. Lett.* **115** (2015) 212001 [`1505.07863`].

[24] Particle Data Group collaboration, *Review of particle physics*, *Phys. Rev. D* **110** (2024) 030001.

[25] RBC, UKQCD collaboration, *Direct CP violation and the* $\Delta I = 1/2$ *rule in* $K \to \pi\pi$ *decay from the standard model*, *Phys. Rev. D* **102** (2020) 054509 [`2004.09440`].

[26] RBC, UKQCD collaboration, $\Delta I$*=3/2 and* $\Delta I$*=1/2 channels of* $K{\to}\pi\pi$ *decay at the physical point with periodic boundary conditions*, *Phys. Rev. D* **108** (2023) 094517 [`2306.06781`].

[27] RBC, UKQCD collaboration, *Kaon mixing beyond the standard model with physical masses*, *Phys. Rev. D* **110** (2024) 034501 [`2404.02297`].

[28] SWME collaboration, *Kaon BSM B-parameters using improved staggered fermions from* $N_f = 2+1$ *unquenched QCD*, *Phys. Rev. D* **93** (2016) 014511 [`1509.00592`].

[29] RBC, UKQCD collaboration, *Domain wall QCD with physical quark masses*, *Phys. Rev. D* **93** (2016) 074505 [`1411.7017`].

[30] J. Laiho and R.S. Van de Water, *Pseudoscalar decay constants, light-quark masses, and* $B_K$ *from mixed-action lattice QCD*, *PoS* **LATTICE2011** (2011) 293 [`1112.4861`].

[31] BMW collaboration, *Precision computation of the kaon bag parameter*, *Phys. Lett. B* **705** (2011) 477 [`1106.3230`].

[32] A.J. Buras, D. Guadagnoli and G. Isidori, *On* $\epsilon_K$ *Beyond Lowest Order in the Operator Product Expansion*, *Phys. Lett. B* **688** (2010) 309 [`1002.3612`].

[33] RBC, UKQCD collaboration, *Long distance contribution to the $K_L - K_S$ mass difference*, *Phys. Rev. D* **88** (2013) 014508 [1212.5931].

[34] RBC, UKQCD collaboration, *Calculating the $K_L - K_S$ mass difference and $\epsilon_K$ to sub-percent accuracy*, *PoS* **LATTICE2013** (2014) 397 [1402.2577].

[35] J. Brod, M. Gorbahn and E. Stamou, *Standard-Model Prediction of $\epsilon_K$ with Manifest Quark-Mixing Unitarity*, *Phys. Rev. Lett.* **125** (2020) 171803 [1911.06822].

[36] A.J. Buras and D. Guadagnoli, *Correlations among new CP violating effects in $\Delta F = 2$ observables*, *Phys. Rev. D* **78** (2008) 033005 [0805.3887].

[37] J. Brod and M. Gorbahn, *$\epsilon_K$ at Next-to-Next-to-Leading Order: The Charm-Top-Quark Contribution*, *Phys. Rev. D* **82** (2010) 094026 [1007.0684].

[38] SWME collaboration, S. Jwa, W. Lee et al. in preparation.

[39] T. Bhattacharya, B.J. Choi, R. Gupta, Y.-C. Jang, S. Jwa, S. Lee et al., *Improved data analysis on two-point correlation function with sequential Bayesian method*, *PoS* **LATTICE2021** (2021) 136 [2204.05848].

[40] LANL-SWME collaboration, *Leptonic decays of $B_{(s)}$ and $D_{(s)}$ using the OK action*, *PoS* **LATTICE2019** (2020) 050 [2002.04755].

[41] LANL/SWME collaboration, *Semileptonic $B \to D^{(*)}\ell\nu$ Decay Form Factors using the Oktay-Kronfeld Action*, *PoS* **LATTICE2019** (2020) 056 [2003.09206].

[42] LANL/SWME collaboration, *Update on $B \to D^*\ell\nu$ form factor at zero-recoil using the Oktay-Kronfeld action*, *PoS* **LATTICE2018** (2018) 283 [1812.07675].

[43] LANL-SWME collaboration, *Calculation of $\bar{B} \to D^*\ell\bar{\nu}$ form factor at zero recoil using the Oktay-Kronfeld action*, *EPJ Web Conf.* **175** (2018) 13012 [1711.01786].

[44] LANL-SWME collaboration, *Improvement of heavy-heavy current for calculation of $\bar{B} \to D^{(*)}\ell\bar{\nu}$ form factors using Oktay-Kronfeld heavy quarks*, *EPJ Web Conf.* **175** (2018) 14010 [1711.01777].

[45] LANL-SWME collaboration, *Improvement of heavy-heavy and heavy-light currents with the Oktay-Kronfeld action*, *Phys. Rev. D* **105** (2022) 034509 [2001.05590].

[46] T. Bhattacharya et al., *Progress report on testing robustness of the Newton method in data analysis on 2-point correlation function using a MILC HISQ ensemble*, *PoS* **LATTICE2023** (2023) 155 [2401.01584].

[47] LANL-SWME collaboration, *Current progress on the semileptonic form factors for $\bar{B} \to D^*\ell\bar{\nu}$ decay using the Oktay-Kronfeld action*, *PoS* **LATTICE2023** (2023) 245 [2401.01561].